

## Development and Performance Evaluation of a Box-type Absorber Solar Air Collector for Crop Drying

B.O. Bolaji

Department of Mechanical Engineering, Federal University of Technology,  
P.M.B. 704, Akure, Nigeria

---

**Abstract:** A box-type absorber solar air collector was designed for use in Ado-Ekiti, Nigeria on latitude  $7.5^{\circ}$  N and constructed with materials that are readily available in the local market. The performance of solar collector with the dryer was evaluated in the month of August. The results show that high temperature can be achieved in the dryer with the use of the box-type absorber collector. The maximum average temperature obtained (during the daylight) inside the collector and drying chamber were  $64.0$  and  $57.0^{\circ}\text{C}$ , respectively, while the maximum ambient temperature observed was  $33.5^{\circ}\text{C}$ . The heating temperature inside the dryer was higher than the ambient temperature by an average of  $15.3^{\circ}\text{C}$  ( $50.7\%$ ) throughout the daylight. Comparison between the performance of this system and that of the other systems with different types of absorber shows that this system is more efficient. During the test a maximum collector efficiency of  $60.5\%$  was obtained in the system.

**Key words:** Solar energy, solar air collector, box-type absorber, dryer

---

### INTRODUCTION

Among the various types of clean energy, special attention has been given to solar energy because it is freely available. The utilization of solar energy is important in developing nations where electrical energy is expensive and energy production is too low to meet requirements. Solar energy is the driving force behind several of the renewable forms of energy. Solar energy is an ideal alternative source of energy because it is abundant and inexhaustible<sup>[1]</sup>.

The use of the sun's energy for drying has been in practice since man set his eyes on the sun. However, the old practice of simply spreading the items in the open had proved very unsatisfactory, hence the search for alternative methods. Artificial dryers have long been in existence; some of them powered electrically or by natural fuels. The ever-rising cost of electricity and natural fuels have kept the operating cost of these dryers rising and indication is that the trend will continue<sup>[2]</sup>. Over the year, interest has developed on solar powered dryers to discover their potential for drying purposes. Because of the diffuse nature of solar radiation, the efficiency of solar air collectors is not very high thus putting a limit to their use<sup>[2]</sup>.

Therefore, the design of the flow duct and heat transfer surface of solar air collectors should be executed with the objective of achieving a high efficiency with low friction losses. A number of investigators have studied air collectors with different configurations. Hamid and Beckman<sup>[3]</sup> and Neepner<sup>[4]</sup> have studied the matrix type air

collector. A detailed theoretical parametric analysis of a single-pass corrugated bare plate solar air collector has been made by Choudhury *et al.*,<sup>[5]</sup> Han<sup>[6]</sup> and Ligrani and Moffat<sup>[7]</sup> have investigated the effect of different geometries of artificial roughness on the heat transfer and friction factor in duct flows. Their analyses and correlations were based on the correlation development by Webb *et al.*<sup>[8]</sup>, who related the friction coefficient to the wall similarity and the heat transfer coefficient to the heat-momentum transfer analogy of flow over a rough surface.

Subsequently, Prasad and Saini<sup>[9]</sup> developed expressions for the heat transfer and friction factor for a fully developed turbulent flow in a solar air heater duct, which was artificially roughened using small diameter wires with various relative roughness heights and pitches. The finned absorber for the air collector was also studied by Liu *et al.*<sup>[10]</sup>, who demonstrated that extended surfaces on the absorber plate caused an increase in heat transfer coefficient. Ong<sup>[11]</sup> presented a simple matrix inversion method of solution that obviated the need of complex algebraic manipulation of energy equations for different designs of air collectors. The designs studied were distinguished by: air flow between the top glass and the absorber plate; air flow between the absorber and the bottom plate.

This study presents a report on the development and performance evaluation of a box-type absorber solar air collector for crop drying. The box-type absorber is used with the aim of increasing the heat transfer area exposed to the flowing air through the collector in order to achieve

high temperature and high efficiency with low friction losses in the system.

**MATERIALS AND METHODS**

**Theoretical Considerations:** Assumptions for the energy balance equations are as follows:

- Uniform temperature distribution across the width of the absorber plate and of the back plate;
- Uniform distribution of the air flow along the collector channels;
- The physical properties of the following air are independent of temperature and pressure;
- Only steady states are considered and the energy stored in the components is neglected;
- All convective heat transfer coefficients between the collector components and flowing air are equal and constant;
- The temperature of the flowing air is uniform over the collector cross-sectional area.

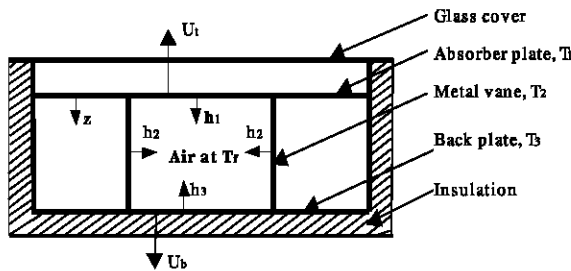


Fig. 1: A schematic of a box-type absorber solar air collector

As shown in Fig. 1, the collector absorbing-surface receives the energy transmitted through the glazing system. The received energy is transferred by convection to the air flowing through the channels; by radiation to the glazing and back plate; by conduction to the metal vanes. The energy balance equations for the collector components are as follows:

For absorber plate:

$$U_t (T_1 - T_a) + h_1(T_1 - T_f) + h_1(T_1 - T_2) + (N/A_c) [-KA(dT_1/dz)]_{z=0} = S \quad (1)$$

For back plate:

$$h_1 (T_1 - T_2) + (N/A_c)[-KA(dT_2/dz)]_{z=D} = h_3(T_3 - T_f) + U_b(T_3 - T_a) \quad (2)$$

For metal vanes:

$$\int_{z=0}^{z=D} 2h_2 l (T_2 - T_f) dz = [-KA (dT_2/dz)]_{z=0} - [-KA(dT_2/dz)]_{z=D} \quad (3)$$

For air flow passage:

$$h_1 (T_1 - T_f) + (N/A_c) \int_{z=0}^{z=D} 2h_2 l (T_2 - T_f) dz + h_3 (T_3 - T_f) = Q_a \quad (4)$$

Where: N = the number of metal vanes per meter of width

A = cross section of the metal vane (m<sup>2</sup>)

A<sub>c</sub> = the area of the collector i.e.

A<sub>c</sub> = W x L<sub>c</sub> (m<sup>2</sup>)

W = the collector width (m)

Solving the differential part of Eq. 1 with some rearranging yields

$$S = [U_t + h_1 + h_1 + F_1(\cosh mD)]T_1 - [(h_1 + F_1(\cosh mD) - F_1]T_f - (h_1 + F_1)T_3 - U_t T_a \quad (5)$$

From Eq. 5, the absorbing surface temperature can be written as

$$T_1 = [U_t + h_1 + h_1 + F_1(\cosh mD)]^{-1} \{ (h_1 + F_1)T_3 + [h_1 + F_1(\cosh mD) - F_1]T_f + U_t T_a + S \} \quad (6)$$

Subtracting T<sub>f</sub> from the light-hand and left-hand sides of Eq. 6 yields

$$T_1 - T_f = F_2^{-1} [ F_3(T_3 - T_f) - U_t(T_f - T_a) + S ] \quad (7)$$

where the factors F<sub>1</sub>, F<sub>2</sub> and F<sub>3</sub> are given as follows:

$$F_1 = (N/A_c)[(2h_2 l k A)^{1/2} / \sinh mD] = (N/A_c)C_1 \quad (8)$$

$$F_2 = U_t + h_1 + h_1 + F_1(\cosh mD) \quad (9)$$

$$F_3 = h_1 + F_1 \quad (10)$$

Where:

$$C_1 = [(2h_2 l k A)^{1/2} / \sinh mD] \quad (11)$$

Similarly, solving the deferential part of Eq. 12 with some rearranging yield

$$(h_1 + F_1)(T_1 - T_f) - [h_1 + F_1(\cosh mD) + h_3 + U_b](T_3 - T_f) - U_b(T_f - T_a) = 0 \quad (12)$$

Eq. 12 can be simplified:

$$F_3(T_1 - T_f) - F_4(T_3 - T_f) - U_b(T_f - T_a) = 0 \quad (13)$$

$$\text{where } F_4 = h_1 + F_1(\cosh mD) + h_3 + U_b \quad (14)$$

Equation 7 and 13 can be solved algebraically and the final results are given as follows:

$$(T_1 - T_f) = [(F_3 U_b + U_b F_4) / (F_3^2 - F_2 F_4)] (T_f - T_a) - [ F_4 / (F_3^2 - F_2 F_4) ] S \quad (15)$$

$$(T_3 - T_f) = [(F_2 U_b + U F_3) / (F_3^2 - F_2 F_4)] (T_f - T_a) - [F_3 / (F_3^2 - F_2 F_4)] S \quad (16)$$

Substituting Eq. 3 into 4 and rearranging of terms gives the useful heat which can be taken from the collector as

$$Q_a = F_5(T_1 - T_f) + F_6(T_3 - T_f) \quad (17)$$

where

$$F_5 = h_1 + F_1[(\cosh mD) - 1] \text{ and } F_6 = h_3 + F_1[(\cosh mD) - 1] \quad (18)$$

Finally, substituting Eq. 15 and 16 into Eq. 17 yields

$$Q_a = [(F_4 F_5 + F_3 F_6) / (F_2 F_4 - F_3^2)] \{S - [F_5(U_b F_3 + U F_4) + F_6(U_b F_2 + U F_3)] / (F_4 F_5 + F_3 F_6)\} (T_f - T_a) \quad (19)$$

Eq. 19 is similar to the general expression for the useful heat from the collector Eq. 20, given by Duffie and Beckman<sup>[12]</sup>

$$Q_a = F^* [S - U_L (T_f - T_a)] \quad (20)$$

Where:

$$F^* = (F_4 F_5 + F_3 F_6) / (F_2 F_4 - F_3^2) \\ U_L = [F_5(U_b F_3 + U F_4) + F_6(U_b F_2 + U F_3)] / (F_4 F_5 + F_3 F_6) \quad (21)$$

Therefore, the above parameters can be used to determine the collector heat removal factor  $F_{Rc}$ , which is used to investigate the collector performance as a function of the inlet temperature.

**Determination of pressure drop and efficiency:** For the laminar flow region, Heaton's empirical correlation<sup>[13]</sup> was employed to determine the Nusselt number for laminar flow between two parallel plates with one side insulated and the other subjected to a constant heat flux:

$$Nu = Nu_{\infty} + \{a[\text{RePr}(D_h / l_c)]^n\} / \{l_c + b[\text{RePr}(D_h / l_c)]^n\} \quad (22)$$

where the constants a, b, c, n and  $Nu_{\infty}$  are given by Ong<sup>[11]</sup> for  $\text{Pr} = 0.7$ .

In the turbulent flow region, Nusselt's correlation<sup>[13]</sup> was employed:

$$Nu = 0.036 \text{Re}^{0.8} \text{Pr}^{1/3} (D_h / l_c)^{0.055} \quad (23)$$

where  $D_h$  is the equivalent diameter in the given case. The expression for the pressure drop through the collector, is given as:

$$\Delta P = \rho C_f (l_c / D_h) (\frac{1}{2} V^2) \quad (24)$$

where  $C_f$  is the friction coefficient for a channel with smooth walls and can be obtained from a Moody Chart<sup>[14]</sup> and  $V$  is the average velocity through the collector channel.

Finally, the collector day-long efficiency can be defined as:

$$\eta_{\text{day}} = (\sum_{\text{day}} Q_u) / (\sum_{\text{day}} I_T) \quad (25)$$

where  $I_T$  is the incident radiation during the day

**The Experimental set-up:** The solar dryer with box-type absorber collector was constructed using the materials that are easily obtainable from local market. Figure.2 shows the diagram of the solar crop dryer. The dryer has four main features viz: the box-type absorber solar air collector, the drying chamber, the drying rack and the chimney.

**Box-type absorber air collector:** The frame absorber is made of aluminium 2 mm thick, painted black and it consists of air flow channels enclosed by an upper absorbing plate, a back plate and metal vanes. The effective area of the collector is 0.412 m<sup>2</sup>. It has heat insulation lining made from foam material of about 40 mm thick. The window is covered with transparent glass of thickness 4 mm. One end of the collector has an air inlet vent of area 0.084 m<sup>2</sup>, the other end opens to the drying chamber.

**The Drying Chamber and Drying Racks:** The drying chamber houses two drying racks, each with an area of 0.168 m<sup>2</sup> and dept of 100 mm (Fig. 3). The racks are made of wooden frame with wire gauze used to construct the bottom so as to allow free air flow, through the produce to be dried and out through the chimney. The drying chamber is also lined with foam insulation material 4 mm thick to prevent loss of heat.

**The chimney:** It is located to the top of the drying chamber. It has a square area of 100 x 100mm (0.01 m<sup>2</sup>) and a height of 350 mm. The height difference between inlet air and exhaust is 1250 mm. This fairly large height difference serves to increase the rate of flow of air through the dryer.

**The Orientation of the Collector:** The box-type absorber collector is orientated in such a way that it receives maximum solar radiation during the desired season of use. According to Adegoke and Bolaji<sup>[15]</sup> the best stationary orientation is due south in the Northern Hemisphere and due north in Southern Hemisphere. In this position the inclination of the collector to the

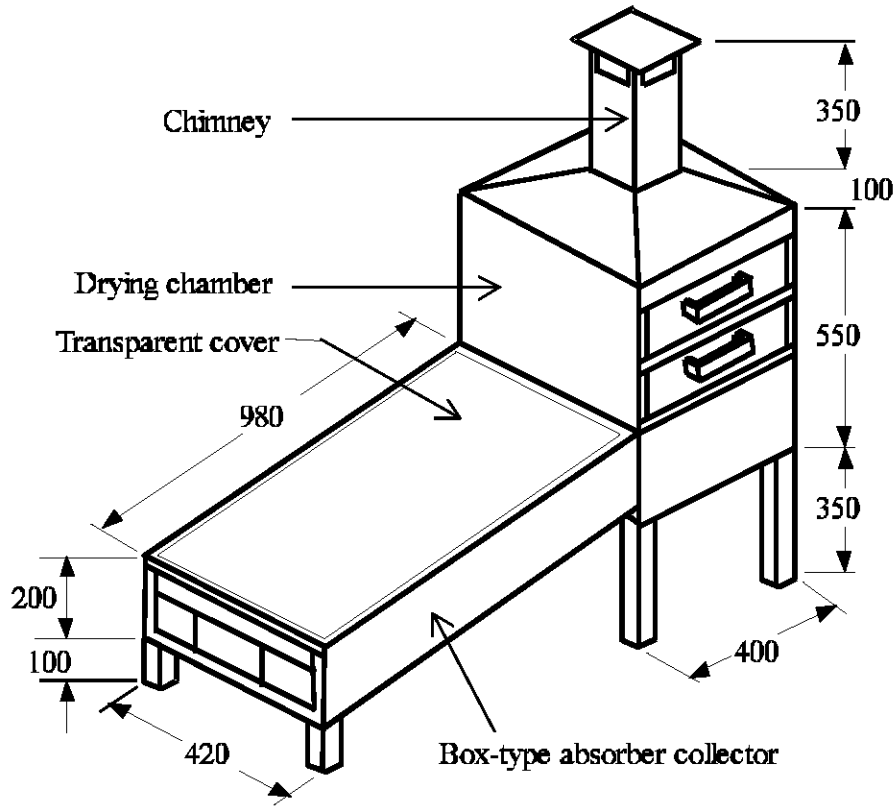


Fig. 2: Solar crop dryer with box-type absorber collector

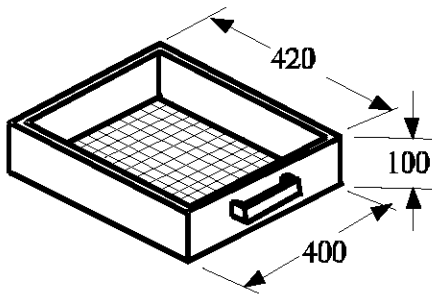


Fig. 3: Drying rack

horizontal plane for the best all year round performance is approximately  $10^\circ$  more than the local geographical latitude. This is the approach used in this work as a tilt angle of  $17.5^\circ$  was used for Ado-Ekiti, Nigeria, location which is on latitude  $7.5^\circ\text{N}$ .

## RESULTS AND DISCUSSION

The box-type absorber solar dryer was tested in the month of August 2003 when its construction was completed. It was used to dry maize and during the drying period, the incident solar radiation intensity was measured using pyranometer. The temperatures of collector inlet air,

collector outlet air, drying chamber, chimney exhaust and ambient air were measured with mercury-in-glass thermometer between the hour of 08.00 and 18.00 h local time. The useful energy gain, the pressure drop through the collector and the collector day-long efficiency were calculated using Eq. 20, 24 and 25 respectively. Figure 4 shows the hourly variation of temperature in the dryer for a typical day, 11th August 2003. The maximum average temperature obtained (during the daylight) inside the collector and drying chamber were  $64.0^\circ\text{C}$  and  $57.0^\circ\text{C}$  respectively, while the maximum ambient temperature observed was  $33.5^\circ\text{C}$ . The heating temperature inside the dryer was higher than the ambient temperature by an average of  $15.3^\circ\text{C}$  (50.7%) throughout the daylight. This is clearly shown by the wide gap between the two curves (Fig. 4). Also, Fig. 5 shows the hourly variation of the solar radiation for the same day. The maximum temperature obtained in the dryer is a function of solar radiation, ambient temperature and the wind speed. This is confirmed when compare Fig. 4 with Fig. 5. In Fig. 4, high temperatures both in the collector and in the drying chamber occurred between 11.00 h and 14.00 h, which correspond to the period of high solar radiation (Fig. 5). During the period of low solar radiation

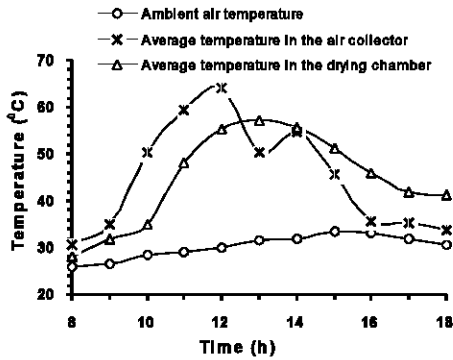


Fig. 4: Hourly variation of air temperature in the solar crop dryer for 11<sup>th</sup> August 2003.

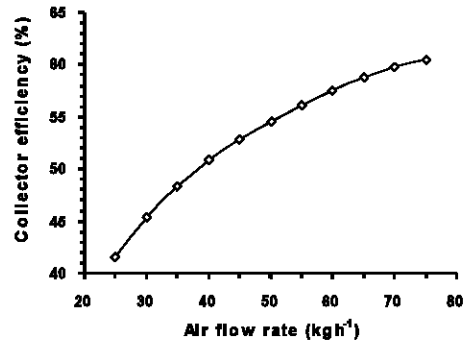


Fig. 7: The collector efficiency versus mass flow rate of the air

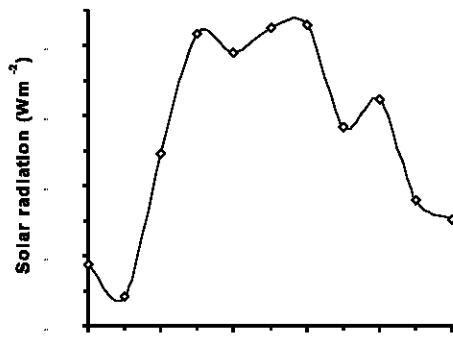


Fig. 5: Hourly variation of solar radiation for 11th August 2003.

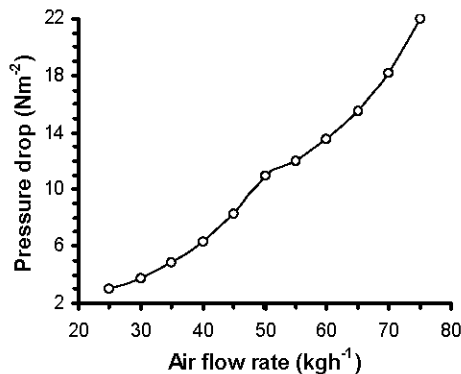


Fig. 6: The pressure drop through the collector at different mass flow rate

between 14.00 hour and 18.00 hour when the air temperature in the collector went down, higher temperature is maintained in the drying chamber. This was possible through the insulation of the drying chamber. This means that drying can take place over a long time in

the dryer. The maximum average air temperature obtained in the collector was 64.0 while 57.3°C was obtained in the drying chamber.

It is clearly shown in Fig. 6 that the pressure drop increases as the mass flow rate increases. This behaviour is related to the dependence of the pressure drop on the air velocity through the collector. The collector day-long efficiency was evaluated and the graph of this efficiency plotted against mass flow rate of the air (Fig. 7). The collector efficiency was found to increase with increasing mass flow rate. This is due to the increase of the convective heat transfer coefficient and the associated decrease of the collector losses. At the lower flow rate (25 kg h<sup>-1</sup>), the collector efficiency was 41.5% and at high flow rate (75 kg h<sup>-1</sup>) the collector efficiency was found to be 60.5%. These results verified the high efficiency of the air collector with a box-type absorber when compare with the work of Awachie<sup>[6]</sup> who studied on solar dryer with flat-plate absorber air collector and Matrawy<sup>[13]</sup> who worked on solar dryer with fin-type absorber air collector. The maximum efficiencies obtained from the two types of collectors are 21 and 36% respectively. The high efficiency of the present work is expected, because in the box-type absorber collector the heat is transferred to the following air via a larger area than in the other cases.

### CONCLUSIONS

This study has shown that the solar air collector with box-type absorber for crop drying can easily be developed and constructed with materials that are readily available in the local market. The test results show that high temperature can be obtained in the solar dryer between the hours of 11.00 and 14.00 local time and temperature above that of ambient air can be maintained in the drying chamber even during the period of low solar

radiation. On the basis of this study, it can be concluded that the temperature of the dryer with box-type absorber collector is always higher than the ambient temperature and drying can take place over a long time.

The efficiency of the solar air collector can be enhanced by using box-type absorber. Comparison between the box-type absorber solar air collector and other types of air collector used by other authors shows that the box-type is more efficient. The maximum efficiency obtained in the box-type absorber system was 60.5% while those of flat-plate absorber and fin-type absorber were 21 and 36% respectively.

### REFERENCES

1. Bolaji, B.O., 2003. The Role of Solar Energy in Preservation of Agricultural Products in Nigeria. In: Adekunle, V., E. Okoko and S. Adeduntan (Eds.). Challenges of Environmental Sustainability in a Democratic Government. Proceedings of 11th Annual Conference of Environment and Behaviour Association of Nigeria (EBAN), pp: 187-193.
2. Ikejiofor, I.D., 1985. Passive solar cabinet dryer for Drying Agricultural Products. In: Awe, O. (Ed.). African Union of Physics. Proceedings of the Workshop on the Physics and Technology of Solar Energy Conversion, University of Ibadan, Nigeria, pp: 157-165.
3. Hamid Y.H. and W.A. Beckman, 1971. Performance of air-cooled radiatively heated screen matrices. *J. Eng. Power*, 93: 221 – 227.
4. Neeper, D.A., 1979. Analysis of matrix air heaters. Proceedings of ISES Congress, Atlanta, Pergamon Press, Elmsford, New York, pp: 298-311.
5. Choudhury, C., S. Andersen and J. Rekstad, 1988. A solar air heater for low temperature applications. *J. Solar Energy*, 40: 335-345.
6. Han, J.C., 1984. Heat transfer and friction in channels with two opposite rib-roughened walls. *J. Heat Transfer*, 106: 774-781.
7. Ligrani, P.M. and R.J. Moffat, 1986. Structure of transitionally rough and fully rough turbulent boundary layers. *J. Fluid Mechanics*, 162: 69-98
8. Webb, R.L., E.R.G. Eckert and R.J. Goldstein, 1971. Heat transfer and friction in tubes with repeated-rib roughness. *Intl. J. Heat and Mass Transfer*, 14: 601-617.
9. Prasad, B.N. and J.S. Saini, 1988. Effect of artificial roughness on heat transfer and friction factor in a solar air heater. *J. Solar Energy*, 41: 555-560.
10. Liu, Y.D., L.A. Diaz and N.V. Suiyanarayana, 1984. Heat transfer enhancement in air heating flat-plate solar collectors. *J. Solar Energy Eng.*, 106: 358-363.
11. Ong, K.S., 1995. Thermal performance of solar air heaters: Mathematical model and solution procedure. *J. Solar Energy*, 55: 93-109.
12. Duffie, J.A. and W.A. Beckman, 1991. *Solar Engineering of Thermal Processes*, 2nd (Edn.). Wiley Interscience, New York.
13. Matrawy, K.K., 1998. New derivation and analysis for a combined solar storage system coupled with a finned absorber air collector. *J. Energy Conversion and Management*, 38: 861-869.
14. Massey, B.S., 1975. *Mechanics of Fluid*. 3rd (Edn.). Van Nostrand Reinhold.
15. Adegoke, C.O. and B.O. Bolaji, 2000. Performance evaluation of solar-operated thermosyphon hot water system in Akure. *Intl. J. Eng. Eng. Technol.*, 2: 35-40.
16. Awachie, I.R.N., 1985. Design, Construction and Evaluation of a Solar Drier in the Nsukka Environment. In: Awe, O., (Edn.). African Union of Physics. Proceedings of the Workshop on the Physics and Technology of Solar Energy Conversion, University of Ibadan, Nigeria, pp: 145-155.